

Identifying Adversarially Attackable and Robust Samples

Vyas Raina

ALTA Institute, University of Cambridge

vr313@cam.ac.uk

Mark Gales

ALTA Institute, University of Cambridge

mjfg@cam.ac.uk

Abstract

This work proposes a novel perspective on adversarial attacks by introducing the concept of sample attackability and robustness. Adversarial attacks insert small, imperceptible perturbations to the input that cause large, undesired changes to the output of deep learning models. Despite extensive research on generating adversarial attacks and building defense systems, there has been limited research on understanding adversarial attacks from an input-data perspective. We propose a deep-learning-based method for detecting the most attackable and robust samples in an unseen dataset for an unseen target model. The proposed method is based on a neural network architecture that takes as input a sample and outputs a measure of attackability or robustness. The proposed method is evaluated using a range of different models and different attack methods, and the results demonstrate its effectiveness in detecting the samples that are most likely to be affected by adversarial attacks. Understanding sample attackability can have important implications for future work in sample-selection tasks. For example in active learning, the acquisition function can be designed to select the most attackable samples, or in adversarial training, only the most attackable samples are selected for augmentation¹.

1. Introduction

Deep learning models have achieved remarkable success across a wide range of tasks and domains, including image classification [10] and natural language processing [14]. However, these models are also susceptible to adversarial attacks [8], where small, imperceptible perturbations to the input can cause large, undesired changes to the output of the model [12, 25, 33]. Extensive research has been conducted on generating adversarial attacks and building defense systems [2, 3], such as detection [11, 22, 26–28] or adversarial training [1, 20, 21]. However, little or no work has sought to understand adversarial attacks from an input-data perspec-

ive. In particular, it is unclear why some samples are more susceptible to attacks than others. Some samples may require a much smaller perturbation for a successful attack, while others may be more robust and require much larger perturbations. Determining the *attackability* of samples can have important implications for various tasks, such as active learning [23, 30] and adversarial training. In the field of active learning, adversarial perturbation sizes can be used by the acquisition function to select the most useful/uncertain samples for training [4, 24]. Similarly, adversarial training can be made more efficient by augmenting with adversarial examples for only the most attackable samples to avoid unnecessarily scaling training times.

This work defines the notion of sample attackability, where the smallest perturbation size to change a sample’s output prediction is used as a measure of the sample’s attackability. Moreover, this work also proposes a simple deep-learning based method to detect the most attackable and robust samples. The attackability detector is evaluated on an unseen dataset, for an unseen target model. Further, the attackability detector is evaluated with an unmatched adversarial attack method; i.e. the detector is trained using perturbation sizes defined by the simple Finite Gradient Sign Method (FGSM) attack [8], but evaluated on sample perturbation sizes calculated using the more powerful Project Gradient Descent (PGD) attack method [18]. The deep-learning based attackability detector is also compared to alternative uncertainty [5] based detectors.

Overall, the contribution of this work is to introduce the concept of sample attackability and sample robustness. This has applications for various sample-selection tasks such as in active learning or can be applied to augmentation based adversarial training systems. The deep-learning based detector proposed by this work is found to be effective in identifying the most attackable and robust samples.

2. Related Works

Understanding adversarial samples: A range of hypotheses exist for explaining the existence of adversarial examples. These explanations are either model/architecture-orientated or from an input data per-

¹Code available at: https://github.com/rainavyas/img_attackability

spective. For understanding sample *attackability*, it is more useful to consider explanations from the data perspective. Initial explanations [9, 31] argued that adversarial examples lie in large and continuous *pockets* of the data manifold (low-probability space), which can be easily accessed. Conversely, it is also hypothesized [32] that adversarial examples simply lie in low variance directions of the data, but this explanation is often challenged [13]. Similarly, many pieces of work [6, 17, 19, 29] argue that adversarial examples lie orthogonal to the data manifold and can so can easily be reached with small perturbations. It can also be argued [7] that adversarial examples are a simple consequence of intricate and high-dimensional data manifolds. Nevertheless, these hypotheses do not offer an explicit explanation or method for identifying individual sample-level susceptibility to adversarial attacks.

Use of adversarial perturbations: In the field of active learning [23, 30], methods have been proposed to exploit adversarial attacks to determine the minimum perturbation size for each sample in a dataset and then the samples are ranked by this perturbation size. The perturbation size is viewed as a proxy for distance to a model’s decision boundary and thus an acquisition function selects the samples with the smallest perturbations for training the model. However, perturbation sizes are very specific to the model being trained, as opposed to contributing to the overall measure of the *attackability* of a sample, agnostic of the model and adversarial attack method. This work seeks to explicitly identify the most attackable and most robust samples in an unseen dataset for an unseen target model.

3. Adversarial Attacks

An untargeted adversarial attack is successful in fooling a classification system, $\mathcal{F}()$, when an input sample \mathbf{x} can be perturbed by a small amount δ to cause a change in the output class,

$$\mathcal{F}(\mathbf{x}) \neq \mathcal{F}(\mathbf{x} + \delta). \quad (1)$$

It is necessary for adversarial attacks to be *imperceptible*, such that adversarial perturbations are not easily detectable/noticeable. For images, an imperceptibility constraint is usually enforced in the l_p norm, with $p = \infty$ being the most popular choice,

$$\|\delta\|_\infty \leq \epsilon, \quad (2)$$

where ϵ is the maximum perturbation size permitted for a change to be deemed appropriately imperceptible. The simplest adversarial attack method for images is Finite Gradient Sign Method (FGSM) [8]. Here, the perturbation direction, δ , is in the direction of the largest gradient of the output loss function, $\mathcal{L}()$, for a model with parameters θ ,

$$\delta = \epsilon \text{sign}(\nabla_{\mathbf{x}} \mathcal{L}(\theta, \mathbf{x}, y)), \quad (3)$$

where the $\text{sign}()$ functions returns $+1$ or -1 , element-wise and y is the target class (or the original predicted class by the model). The Basic Iterative Method (BIM) [16] improves upon the FGSM method, but the most powerful first order image attack method is generally Project Gradient Descent (PGD) [18]. The PGD method adapts the iterative process of BIM to include random initialization and projection. Specifically, an adversarial example \mathbf{x}'_0 is initialized randomly by selecting a point uniformly on the l_∞ ball around \mathbf{x} . Then this adversarial example is updated iteratively,

$$\mathbf{x}'_{i+1} = \prod_{\mathbf{x}+\mathcal{S}} [\mathbf{x}'_i + \alpha \text{sign}(\nabla_{\mathbf{x}} \mathcal{L}(\theta, \mathbf{x}, y))|_{\mathbf{x}=\mathbf{x}'_i}], \quad (4)$$

where \prod denotes the projection operator for mapping back into the space of all acceptable perturbations \mathcal{S} around \mathbf{x} (element-wise clipping to ensure the elements are within the l_∞ ball of size ϵ around \mathbf{x}) and α is a tunable gradient step. The PGD attack can be run for t iterations. The adversarial perturbation, δ is then simply $\delta = \mathbf{x}'_t - \mathbf{x}$.

4. Sample Attackability

Sample attackability aims to understand, *how easy is it* to attack a specific sample. For a specific model, \mathcal{F}_k , we can state a sample, n ’s attackability can be measured directly by the smallest perturbation required to change the classification of the model,

$$\hat{\delta}_n^{(k)} = \min_{\delta} (\mathcal{F}_k(\mathbf{x}_n) \neq \mathcal{F}_k(\mathbf{x}_n + \delta)). \quad (5)$$

Then we can define sample n as *attackable* for model k if the magnitude of the optimal adversarial perturbation is less than a set threshold, $\mathbf{A}_{n,k} = (|\hat{\delta}_n^{(k)}| < \epsilon_a)$, where any sample that is not attackable can be denoted as $\bar{\mathbf{A}}_{n,k}$. Conversely, a sample can be defined as *robust*, if its adversarial perturbation is larger than a set threshold, $\mathbf{R}_{n,k} = (|\hat{\delta}_n^{(k)}| > \epsilon_r)$.

However, it is useful to identify samples that are *universally* attackable/robust, i.e. the definition is agnostic of the model, k , used. We can thus extend the definition for *universality* as follows. A sample, n , is **universally attackable** if,

$$\mathbf{A}_n^{(\mathcal{M})} = \bigcap_{k, \mathcal{F}_k \in \mathcal{M}} \mathbf{A}_{n,k}, \quad (6)$$

where \mathcal{M} is the set of models in consideration. Similarly a sample is **universally robust** if, $\mathbf{R}_n^{(\mathcal{M})} = \bigcap_{k, \mathcal{F}_k \in \mathcal{M}} \mathbf{R}_{n,k}$. The definition of attackability does not explicitly consider the adversarial attack method used to determine the adversarial perturbations. Experiments in Section 6 demonstrate that the rank correlation between different attack methods (FGSM and PGD) is extremely high, suggesting that only the thresholds ϵ_a and ϵ_r have to be adjusted to ensure the same samples are defined as attackable or robust, independent of the attack method used.

5. Attackable and Robust Sample Detection

Section 4 defines attackable ($\mathbf{A}_{n,k}$) and robust ($\mathbf{R}_{n,k}$) samples. This section introduces a deep-learning based method to identify the attackable and robust samples in an unseen dataset, for an unseen target model, \mathcal{F}_t . Let the deep-learning attackability detector have access to a seen dataset, $\{\mathbf{x}_n, y_n\}_{n=1}^N$ and a set of seen models, $\mathcal{M} = \{\mathcal{F}_1, \dots, \mathcal{F}_{|\mathcal{M}|}\}$, such that $\mathcal{F}_t \notin \mathcal{M}$. Each model can be represented as an encoding stage, followed by a classification stage,

$$\mathcal{F}_k(\mathbf{x}_n) = \mathcal{F}_k^{(c1)}(\mathbf{h}_{n,k}), \quad (7)$$

where $\mathbf{h}_{n,k}$ is the output of the model's encoding of \mathbf{x}_n . A separate attackability detector can be trained for each seen model in \mathcal{M} . For a specific seen model, k , we can measure the attackability of each sample using the minimum perturbation size (Equation 5), $\{\delta_n^{(k)}\}_{n=1}^N$. It is useful and efficient to exploit the encoding representation of input images, $\mathbf{h}_{n,k}$, already learnt by each model. Hence, each deep attackability detector, $\mathcal{D}_\theta^{(k)}$, with parameters θ , can be trained as a binary classification task to determine the probability of a sample being attackable for model k , using the encoding at the input,

$$p(\mathbf{A}_{n,k}) = \mathcal{D}_\theta^{(k)}(\mathbf{h}_{n,k}). \quad (8)$$

This work uses a simple, single hidden-layer fully connected network architecture for each detector, \mathcal{D} , such that,

$$\mathcal{D}_\theta(\mathbf{h}) = \sigma(\mathbf{W}_1 \sigma(\mathbf{W}_0 \mathbf{h})), \quad (9)$$

where \mathbf{W}_1 and \mathbf{W}_2 are the trainable parameters and $\sigma()$ is a standard sigmoid function. Now, we have a collection model-specific detectors that we want to use to determine the probability of a sample being attackable for the unseen target model, \mathcal{F}_t . A simple estimate is to use an average over the model-specific detector attackability probabilities,

$$p(\mathbf{A}_{n,t}) \approx \frac{1}{|\mathcal{M}|} \sum_{k, \mathcal{F}_k \in \mathcal{M}} p(\mathbf{A}_{n,k}). \quad (10)$$

However, it is demanding to expect the seen models, \mathcal{M} , specific attackability detectors to accurately estimate the samples that are attackable for \mathcal{F}_t specifically. Hence, instead we can directly aim to estimate the probability of a *universally attackable* sample (defined in Equation 6),

$$p(\mathbf{A}_n^{(\mathcal{M}+t)}) \approx \left[\frac{1}{|\mathcal{M}|} \sum_{k, \mathcal{F}_k \in \mathcal{M}} p(\mathbf{A}_{n,k}) \right]^{\alpha(\mathcal{M})}, \quad (11)$$

where the parameter $\alpha(\mathcal{M})$ models the idea that the probability of universal attackability should decrease with the number of models, i.e. by definition, the number of samples defined as *universally attackable* can only decrease as

number of models in \mathcal{M} increases, as is observed in Figure 1 with the *uni* curve lying below all the model-specific curves. Hence, $\alpha(\mathcal{M}) \geq 1$ and increases with $|\mathcal{M}|$ ².

Similarly, detectors can be trained to determine the probability of a sample being universally robust, $p(\mathbf{R}_n^{(\mathcal{M}+t)})$. As a simpler alternative to a deep attackability detector, uncertainty-based detectors can also be used to identify attackable/robust samples. The simplest form of uncertainty is negative confidence (probability of the predicted class), where it is intuitively expected that the most confident predictions will be for the *robust* samples, $\text{conf}_k(\mathbf{x}) > \rho_r$ and the least confidence samples can be classed as *attackable*, $\text{conf}_k(\mathbf{x}) < \rho_a$.

We can evaluate the performance of the attackability detectors on the unseen target model, $\mathcal{F}_t \notin \mathcal{M}$, using four variations on defining a sample, n as attackable:

1. **all** - the sample is attackable for the unseen target model.

$$\mathbf{A}_{n,t} = (|\hat{\delta}_n^{(t)}| < \epsilon_a). \quad (12)$$

2. **uni** - the sample is universally attackable for the unseen models and the target model.

$$\mathbf{A}_n^{(\mathcal{M}+t)} = \mathbf{A}_{n,t} \cap \mathbf{A}_n^{(\mathcal{M})}. \quad (13)$$

3. **spec** - the sample is attackable for the target model but not universally attackable for the seen models.

$$\mathbf{A}_{n,t}^{\text{spec}} = \mathbf{A}_{n,t} \cap \bar{\mathbf{A}}_n^{(\mathcal{M})}. \quad (14)$$

4. **vspec** - a sample is specifically attackable for the unseen target model only.

$$\mathbf{A}_{n,t}^{\text{vspec}} = \mathbf{A}_{n,t} \cap \left(\bigcap_{k, \mathcal{F}_k \in \mathcal{M}} \bar{\mathbf{A}}_{n,k} \right). \quad (15)$$

As discussed for Equation 11, it is expected that the deep learning-based detectors will perform best in the **uni** evaluation setting.

For an unseen dataset, we can evaluate the performance of attackability detectors using precision and recall, for a selected threshold used to define attackability, e.g., ϵ_a . The precision is $\text{prec} = \text{TP}/\text{TP}+\text{FP}$ and recall is $\text{rec} = \text{TP}/\text{TP}+\text{FN}$, where FP, TP and FN are standard counts for False-Positive, True-Positive and False-Negative. A single value summary is given using the F1-score, $\text{F1} = 2 * (\text{prec} * \text{rec}) / (\text{prec} + \text{rec})$. We can generate a full precision-recall curve by sweeping over all values for the attackability defining threshold (e.g. ϵ_a) and then select the best F1 score.

²An alternative product-based model for universal attackability was considered: $p(\mathbf{A}_n^{(\mathcal{M}+t)}) \approx \left[\prod_{k, \mathcal{F}_k \in \mathcal{M}} p(\mathbf{A}_{n,k}) \right]^{\alpha(\mathcal{M})}$, but empirical results were slightly worse for attackable and robust sample detection.

6. Experiments

6.1. Experimental Setup

Attackability detection experiments are carried out on two standard classification benchmark datasets: Cifar10 and Cifar100 [15]. Cifar10 consists of 50,000 training images and 10,000 test images, uniformly distributed over 10 image classes. Cifar100 is a more challenging dataset, with the same number of train/test images, but distributed over 100 different classes. For both datasets, the training images were randomly separated into a *train* and *validation* set, using a 80-20% split ratio. For training the attackability detectors, direct access was provided to only the validation data and the test data is used to assess the performance.

Four state of the art different model architectures are considered. Model performances are given in Table 1³. Three models (vgg, resnext and densenet) are treated as *seen* models, \mathcal{M} , that the attackability detector has access to during training. The wide-resnet (wrn) model is maintained as an *unseen* model, $\mathcal{F}_t \notin \mathcal{M}$ used only to assess the performance of the attackability detector, as described in Section 5.

Model	Cifar10	Cifar100
vgg-19	93.3	71.8
resnext-29-8-64	96.2	82.5
densenet-121/190-40	87.5	82.7
wrn-28-10	96.2	81.6

Table 1. Model Accuracy (%)

Two adversarial attack types are considered in these experiments: FGSM (Equation 3) and the PGD (Equation 4). The FGSM attack is treated as a *known* attack type, which the attackability detector has knowledge of during training, whilst the more powerful PGD attack is an *unknown* attack type, reserved for evaluation of the detector. In summary, these experiments use three *seen* models, the validation set and FGSM-based attacks to train an attackability detector. This detector is then required to identify robust/attackable samples for an unseen test set and an unseen target model, attacked using either the known FGSM (*matched evaluation*) or PGD (*unmatched evaluation*).

6.2. Results

Initial experiments consider the *matched* evaluation setting. For each *seen* model (vgg, resnext and densenet), the FGSM method is used to determine the minimum perturbation size, $\hat{\delta}_n^{(k)}$, required to successfully attack each sample,

³Saved model parameters, hyper-parameter training details and code for all models is provided as a public repository: <https://github.com/bearpaw/pytorch-classification>

n in the validation dataset for model k (Equation 5). Figure 1 shows (for Cifar100 as an example) the fraction, f of samples that are successfully attacked for each model, as the adversarial attack constraint, ϵ_a is varied: $f = \frac{1}{N} \sum_n \mathbb{1}_{A_{n,k}}$. Based on this distribution, any samples with a perturbation size below $\epsilon_a = 0.05$ are termed *attackable* and any samples with a perturbation size above $\epsilon_r = 0.39$ are termed *robust*. Note that the *uni* curve in Figure 1 shows the fraction of *universally* attackable samples, i.e. these samples are attackable as per all three models (Equation 6).

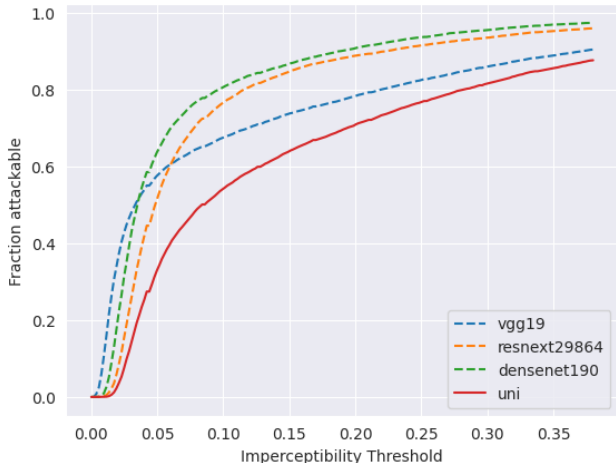


Figure 1. Fraction of *attackable* samples.

Section 5 describes a simple method to train a deep learning classifier to detect robust/attackable samples. Hence, a single layer fully connected network (Equation 9) is trained with *seen* (vgg, resnext, densenet) model’s encodings⁴, using the validation samples in two binary classification settings: 1) detect attackable samples and 2) detect robust samples. The number of hidden layer nodes for each model’s FCN is set to the encoder output size. Training of the FCNs used a batch-size of 64, 200 epochs, a learning rate of 1e-3 (with a factor 10 drop at epochs 100 and 150), momentum of 0.9 and weight decay of 1e-4 with stochastic gradient descent. As described in Section 5, an ensemble of the confidence of the three seen architectures (conf-s) and the confidence of the unseen architecture, wrn, (conf-u) are also used as uncertainty based detectors for comparison to the deep-learning based (deep) attackability/robust sample detector. To better understand the operation of the detectors, Section 5 defines four evaluation settings: all (Equation 12), uni (Equation 13), spec (Equation 14) and vspec (Equation 15). Table 2 shows the best F1 scores for detecting *attackable* samples on the unseen test data for the unseen wrn model, in the matched setting (FGSM attack used to define

⁴Encoding stage for each model defined in: https://github.com/rainavyas/img_attackability/blob/main/src/models/model_embedding.py

perturbation sizes for each sample in the test dataset). Note that the scale of F1 scores can vary significantly between evaluation settings as the prevalence of samples defined as *attackable* in a dataset are different. Table 3 presents the equivalent results for detecting robust samples, where the definitions for each category update to identifying *robust* samples ($\mathbf{R}_{n,k}$). For Cifar10 data, the deep unseen detection method performs the best only in the *uni* evaluation setting for both attackable and robust sample detection. This is perhaps expected due to the deep detection method having been designed for this purpose (Equation 11), whilst for example the *conf seen* detection method has direct access to the target unseen model (wrn) and is able to perform better in the *spec* and *vspec* settings. When evaluation is on *all* attackable/robust samples for wrn, the superior *vspec* and *spec* performances of the uncertainty detectors, allows them to do better overall. However, for Cifar100 data, the deep detection method is able to perform significantly better in every setting other than the *vspec* evaluation setting, which is expected as this detector has no access to the target model and cannot identify samples specifically attackable/robust for the target model (wrn).

Setting		conf-s	conf-u	deep
all	cifar10	0.693	0.681	0.683
	cifar100	0.845	0.851	0.874
uni	cifar10	0.660	0.643	0.682
	cifar100	0.792	0.827	0.831
spec	cifar10	0.239	0.209	0.206
	cifar100	0.263	0.261	0.271
vspec	cifar10	0.010	0.006	0.006
	cifar100	0.018	0.018	0.018

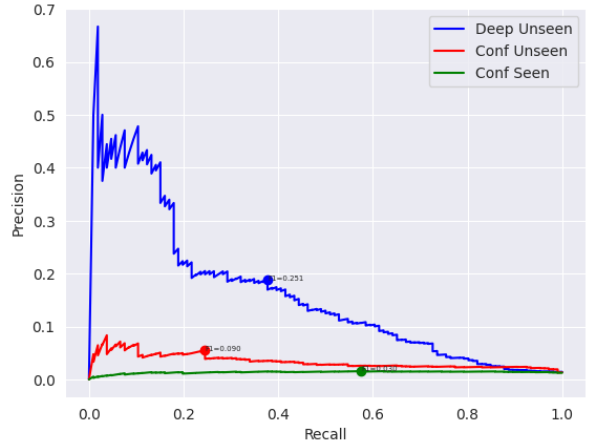
Table 2. Attackable Sample Detection (F1) in matched setting.

Setting		conf-s	conf-u	deep
all	cifar10	0.501	0.502	0.435
	cifar100	0.134	0.161	0.385
uni	cifar10	0.030	0.090	0.251
	cifar100	0.026	0.074	0.565
spec	cifar10	0.486	0.485	0.422
	cifar100	0.119	0.141	0.286
vspec	cifar10	0.300	0.288	0.254
	cifar100	0.042	0.061	0.055

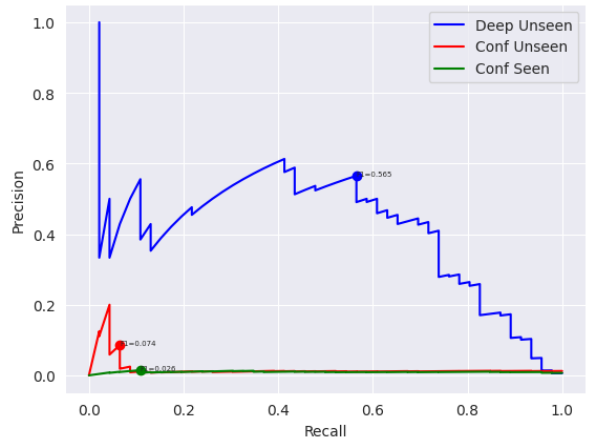
Table 3. Robust Sample Detection in matched setting.

Figure 2 presents the precision-recall curves for detecting robust samples (by sweeping the detection threshold ϵ) in the *uni* evaluation setting, which the deep-learning based

detector has been designed for. It is evident that for a large range of operating points, the deep detection method dominates and is thus truly a useful method for identifying robust samples. Figure 3 presents the equivalent precision-recall curves for detecting attackable samples. Here, although the deep-learning method still dominates, the differences are less significant. Hence, it can be argued that this deep learning-based attackability detector is capable of identifying both attackable and robust samples, but is particularly powerful in detecting robust samples.



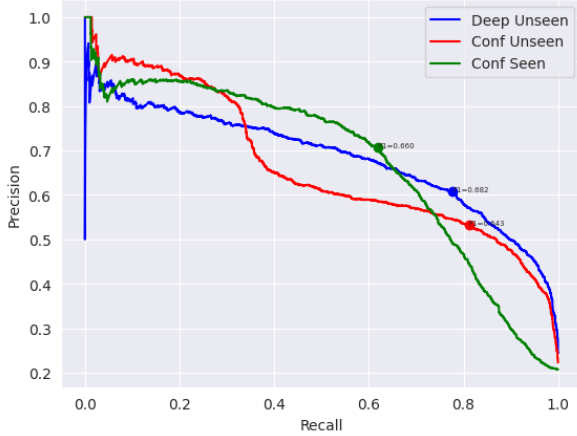
(a) Cifar10



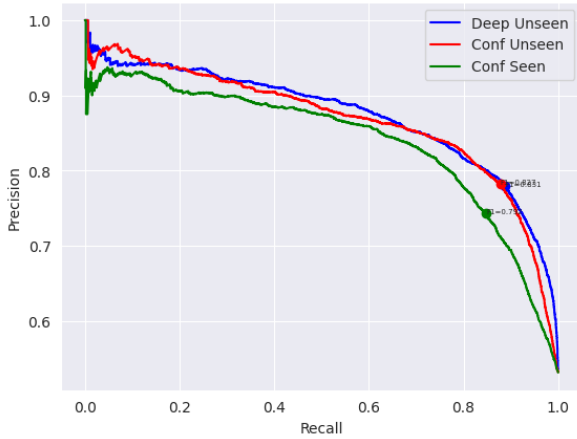
(b) Cifar100

Figure 2. P-R curves for detecting *universal robust* samples.

In the unmatched evaluation setting the aim is to identify the attackable/robust samples in the test data, where the perturbation sizes for each sample are calculated using the more powerful *unknown* PGD attack method (Equation 4). PGD attacks used 8 iterations of the attack loop. Table 4 gives the Spearman rank correlation of samples in the validation set when perturbation sizes, $|\delta_n|$, for each sample, n , are calculated using the known attack, FGSM, or the unknown attack, PGD. For all models, with correlations near



(a) Cifar10



(b) Cifar100

Figure 3. P-R Curves for detecting *universal attackable* samples.

1.0, PGD and FGSM attack methods demonstrate a very strong correlation. This implies that the results from the matched setting should transfer easily to the unmatched setting.

	vgg	resnext	densenet
cifar10	0.840	0.849	0.951
cifar100	0.947	0.900	0.911

Table 4. Spearman rank correlation (PGD, FGSM) perturbations.

Table 5 gives the F1 scores for detecting attackable samples in the unmatched setting and Table 6 gives the equivalent results for detecting robust samples. As the PGD attack is more powerful than the FGSM attack, the definition of the attackable threshold and robustness threshold are adjusted to $\epsilon_a = 0.03$ and $\epsilon_r = 0.10$. The deep unseen detectors once again dominate in the universal evaluation settings (specifically for robust sample detection) and thus, the trends iden-

tified for the matched evaluation setting are maintained in the more challenging unmatched setting. The deep-learning based simple detectors can be viewed as effective methods for identifying attackable/robust samples for an unseen dataset, using an unseen model and attackability defined as per an unknown attack method.

Setting		conf-s	conf-u	deep
all	cifar10	0.694	0.776	0.797
	cifar100	0.886	0.882	0.907
uni	cifar10	0.636	0.754	0.777
	cifar100	0.846	0.871	0.893
spec	cifar10	0.245	0.245	0.261
	cifar100	0.167	0.167	0.167
vspec	cifar10	0.012	0.012	0.012
	cifar100	0.006	0.006	0.006

Table 5. Attackable Sample Detection in unmatched setting.

Setting		conf-s	conf-u	deep
all	cifar10	0.195	0.291	0.146
	cifar100	0.088	0.114	0.307
uni	cifar10	0.008	0.008	0.048
	cifar100	0.005	0.006	0.233
spec	cifar10	0.192	0.288	0.144
	cifar100	0.084	0.113	0.277
vspec	cifar10	0.149	0.221	0.110
	cifar100	0.041	0.055	0.095

Table 6. Robust Sample Detection in unmatched setting.

7. Conclusion

This work proposes a novel perspective on adversarial attacks by introducing the concept of sample attackability and robustness. A sample can be defined as attackable if its minimum perturbation size (for a successful adversarial attack) is less than a set threshold and conversely a sample can be defined as robust if its minimum perturbation size is greater than another set threshold. A deep-learning based attackability detector is trained to identify universally attackable/robust samples for unseen data and an unseen target model. In comparison to uncertainty-based attackability detectors, the deep-learning method performs best, with significant gains for robust sample detection. The understanding of sample attackability and robustness can have important implications for various tasks such as active learning and adversarial training. Future work can explore the significance of attackability on the design of more robust systems.

References

- [1] Tao Bai, Jinqi Luo, Jun Zhao, Bihan Wen, and Qian Wang. Recent advances in adversarial training for adversarial robustness. In Zhi-Hua Zhou, editor, *Proceedings of the Thirtieth International Joint Conference on Artificial Intelligence, IJCAI-21*, pages 4312–4321. International Joint Conferences on Artificial Intelligence Organization, 8 2021. Survey Track. [1](#)
- [2] Battista Biggio and Fabio Roli. Wild patterns: Ten years after the rise of adversarial machine learning. *CoRR*, abs/1712.03141, 2017. [1](#)
- [3] Anirban Chakraborty, Manaar Alam, Vishal Dey, Anupam Chattopadhyay, and Debdeep Mukhopadhyay. Adversarial attacks and defences: A survey. *CoRR*, abs/1810.00069, 2018. [1](#)
- [4] Melanie Ducoffe and Frédéric Precioso. Adversarial active learning for deep networks: a margin based approach. *CoRR*, abs/1802.09841, 2018. [1](#)
- [5] Jakob Gawlikowski, Cedricque Rovile Njietcheu Tassi, Mohsin Ali, Jongseok Lee, Matthias Humt, Jianxiang Feng, Anna M. Kruspe, Rudolph Triebel, Peter Jung, Ribana Roscher, Muhammad Shahzad, Wen Yang, Richard Bamler, and Xiao Xiang Zhu. A survey of uncertainty in deep neural networks. *CoRR*, abs/2107.03342, 2021. [1](#)
- [6] Partha Ghosh, Arpan Losalka, and Michael J. Black. Resisting adversarial attacks using gaussian mixture variational autoencoders. *CoRR*, abs/1806.00081, 2018. [2](#)
- [7] Justin Gilmer, Luke Metz, Fartash Faghri, Samuel S. Schoenholz, Maithra Raghu, Martin Wattenberg, and Ian J. Goodfellow. Adversarial spheres. *CoRR*, abs/1801.02774, 2018. [2](#)
- [8] Ian J. Goodfellow, Jonathon Shlens, and Christian Szegedy. Explaining and harnessing adversarial examples, 2014. [1](#), [2](#)
- [9] Shixiang Gu and Luca Rigazio. Towards deep neural network architectures robust to adversarial examples, 2014. [2](#)
- [10] Zhengyu He. Deep learning in image classification: A survey report. In *2020 2nd International Conference on Information Technology and Computer Application (ITCA)*, pages 174–177, 2020. [1](#)
- [11] Dan Hendrycks and Kevin Gimpel. Visible progress on adversarial images and a new saliency map. *CoRR*, abs/1608.00530, 2016. [1](#)
- [12] Ngoc Dung Huynh, Mohamed Reda Bouadjenek, Imran Razzak, Kevin Lee, Chetan Arora, Ali Hassani, and Arkady Zaslavsky. Adversarial attacks on speech recognition systems for mission-critical applications: A survey, 2022. [1](#)
- [13] Rauf Izmailov, Shridatt Sugrim, Ritu Chadha, Patrick McDaniel, and Ananthram Swami. Enablers of adversarial attacks in machine learning. In *MILCOM 2018 - 2018 IEEE Military Communications Conference (MILCOM)*, pages 425–430, 2018. [2](#)
- [14] Diksha Khurana, Aditya Koli, Kiran Khatter, and Sukhdev Singh. Natural language processing: State of the art, current trends and challenges. *CoRR*, abs/1708.05148, 2017. [1](#)
- [15] Alex Krizhevsky. Learning multiple layers of features from tiny images. pages 32–33, 2009. [4](#)
- [16] Alexey Kurakin, Ian J. Goodfellow, and Samy Bengio. Adversarial machine learning at scale. *CoRR*, abs/1611.01236, 2016. [2](#)
- [17] Hyeungill Lee, Sungyeob Han, and Jungwoo Lee. Generative adversarial trainer: Defense to adversarial perturbations with GAN. *CoRR*, abs/1705.03387, 2017. [2](#)
- [18] Aleksander Madry, Aleksandar Makelov, Ludwig Schmidt, Dimitris Tsipras, and Adrian Vladu. Towards deep learning models resistant to adversarial attacks, 2017. [1](#), [2](#)
- [19] Dongyu Meng and Hao Chen. Magnet: a two-pronged defense against adversarial examples. *CoRR*, abs/1705.09064, 2017. [2](#)
- [20] Awais Muhammad and Sung-Ho Bae. A survey on efficient methods for adversarial robustness. *IEEE Access*, 10:118815–118830, 2022. [1](#)
- [21] Zhuang Qian, Kaizhu Huang, Qiu-Feng Wang, and Xu-Yao Zhang. A survey of robust adversarial training in pattern recognition: Fundamental, theory, and methodologies, 2022. [1](#)
- [22] Vyas Raina and Mark Gales. Residue-based natural language adversarial attack detection. In *Proceedings of the 2022 Conference of the North American Chapter of the Association for Computational Linguistics: Human Language Technologies*. Association for Computational Linguistics, 2022. [1](#)
- [23] Pengzhen Ren, Yun Xiao, Xiaojun Chang, Po-Yao Huang, Zhihui Li, Xiaojiang Chen, and Xin Wang. A survey of deep active learning. *CoRR*, abs/2009.00236, 2020. [1](#), [2](#)
- [24] Dongyu Ru, Jiangtao Feng, Lin Qiu, Hao Zhou, Mingxuan Wang, Weinan Zhang, Yong Yu, and Lei Li. Active sentence learning by adversarial uncertainty sampling in discrete space. In *Findings of the Association for Computational Linguistics: EMNLP 2020*, pages 4908–4917, Online, Nov. 2020. Association for Computational Linguistics. [1](#)
- [25] Alex Serban, Erik Poll, and Joost Visser. Adversarial examples on object recognition: A comprehensive survey. *CoRR*, abs/2008.04094, 2020. [1](#)
- [26] Uri Shaham, James Garritano, Yutaro Yamada, Ethan Weinberger, Alex Cloninger, Xiuyuan Cheng, Kelly Stanton, and Yuval Kluger. Defending against adversarial images using basis functions transformations, 2018. [1](#)
- [27] Chaomin Shen, Yaxin Peng, Guixu Zhang, and Jinsong Fan. Defending against adversarial attacks by suppressing the largest eigenvalue of fisher information matrix. *CoRR*, abs/1909.06137, 2019. [1](#)
- [28] Lewis Smith and Yarin Gal. Understanding measures of uncertainty for adversarial example detection, 2018. [1](#)
- [29] Yang Song, Taesup Kim, Sebastian Nowozin, Stefano Ermon, and Nate Kushman. Pixeldefend: Leveraging generative models to understand and defend against adversarial examples. *CoRR*, abs/1710.10766, 2017. [2](#)
- [30] Li-Li Sun and Xi-Zhao Wang. A survey on active learning strategy. In *2010 International Conference on Machine Learning and Cybernetics*, volume 1, pages 161–166, 2010. [1](#), [2](#)
- [31] Christian Szegedy, Wojciech Zaremba, Ilya Sutskever, Joan Bruna, Dumitru Erhan, Ian Goodfellow, and Rob Fergus. Intriguing properties of neural networks, 2013. [2](#)

- [32] Thomas Tanay and Lewis D. Griffin. A boundary tilting perspective on the phenomenon of adversarial examples. *CoRR*, abs/1608.07690, 2016. [2](#)
- [33] Wei Emma Zhang, Quan Z. Sheng, and Ahoud Alhazmi. Generating textual adversarial examples for deep learning models: A survey. *CoRR*, abs/1901.06796, 2019. [1](#)